FULL SCALE TEST OF ALL-STEEL BUCKLING RESTRAINED BRACES

Ning Ma[1], Bin Wu[2], Junxian Zhao[1], Hui Li[2], Jinping Ou[*3], Weibiao Yang[4]

[1] *PhD Candidate , School of Civil Engineering, Harbin Institute of Technology, Harbin, China*
[2] *Professor, School of Civil Engineering, Harbin Institute of Technology, Harbin, China*
[3] *Correspondence Author, Professor, School of Civil Engineering, Dalian University of Technology, Dalian, China*
[4] *Professor, China Institute of Building Standard Design and Research, Beijing, China*
Email: mning_hit@126.com, bin.wu@hit.edu.cn, storebelly@163.com, lihui@hit.edu.cn, oujinping@hit.edu.cn, yang-weibiao@vip.sina.com

ABSTRACT :

Buckling-restrained braces (BRBs) are widely used seismic response-controlling members with excellent energy dissipation capacity without buckling at design deformation. However, the property of all-steel BRBs with cruciform cross section encased in a square steel tube remains insufficiently studied. In this paper, the properties of this kind of BRBs, which were used in two office buildings in Beijing, were examined by full-scale test. First, initial design was done according to the client's requirement. Then, two full-scale specimens were tested under uniaxial quasi-static cyclic loading. The test results indicate that there should be no welding in yielding portion of the core. Finally, the full-scale subassemblage test was done with an improved BRB and gusset plates installed in a frame. The result shows that the brace exhibited high energy dissipation capacity and stable hysteretic characteristic. According to the results from above tests, some important issues are summarized to provide advices for practical applications.

KEYWORDS: all-steel buckling-restrained brace, full-scale test, cruciform cross section, hysteretic behavior

1. INTRODUCTION

As a damage-controlling member, buckling restrained braces (BRBs) offer not only stiffness but also excellent energy dissipation through uniformly distributed yielding on the cross section along the whole core plate. Typical BRB consists of an inner steel core surrounded by an outer encasing member. The former carries the axial load, while the later provides lateral support to the core and prevents it from buckling in compression at the target lateral displacement.

The concept of BRB was first proposed by Kimura et al. (1976). Because of their outstanding seismic behavior, BRBs have been widely used in Japan (Xie, 2006; Iwata and Murai, 2006), USA (Black et al., 2002) and Taiwan (Tsai et al., 2003). According to the restraining members, BRBs are classified in two types: one is restrained by steel tubes filled with concrete or mortar, and the other by pure steel tubes, i.e., all-steel BRBs. The all-steel BRBs have such merits as light weight, simple construction and short manufacture period. The all-steel BRBs with cruciform cross section encased in a square steel tube have been installed in two six-floor office buildings of Tonghui Jiayuan in Beijing. The cruciform cross section can be designed to offer larger force or greater local buckling resistance than the rectangular cross section. However, in the available literature (Xie, 2006) the seismic behavior of this type of BRBs has not yet found experimental studies. Series full-scale tests were conducted to ensure the safety of application of all-steel braces to Tonghui Jiayuan. This paper describes the construction development and hysteretic tests of the all-steel BRBs.

Two office buildings of Tonghui Jiayuan are composite frame structures composed of concrete filled steel tube columns and steel beams. To improve its seismic performance, all-steel BRBs were installed in the four frames of each building from the first to the fourth story. The span of the framework is 6.8m, and the height of the stories is 3.5m except for the first story, the height of which is 3.6m. The prototype of the BRB installed in the first floor is research in this paper.

2. BRB SPECIMEN

2.1. Design Requirement for Specimen

In the real structure, the BRB with the overall length of 2337mm, was installed in an inverted chevron pattern with a horizontal angle of 46.43 degree. The design axial deformation was 24mm, corresponding to 1.0% story drift, and the design yielding force was 1500kN.

2.2. Construction of the BRB

The steel of the BRBs was Q235 grade. The cruciform core member consisted of three rectangle steel plates connected by welding. The yielding stress was 210Mpa obtained from material test. Because of the limited space of loading frame, in the uniaxial tests to be described in section 3, we had to keep only a short part of the end plates of the specimens, but the core and transition area was left the same as those in the real structure, as shown in Fig.1. But for subassemblage test, the specimen was exactly the same as that in the real structure, as shown in Fig.2. The BRBs used in the uniaxial test are designated as BRB-1 and BRB-2, and that in the subassemblage test as BRB-3.

At each end of the tube there was a stiffening hoop to enhance the restraining effect for the core member. The core was connected to the end plate by penetrated butt welds. Four reinforcing ribs covered the transition area at each of four sides to keep this area within the elastic range. To prevent the outer tube from slipping down when the core is under the axial force and to make sure the tube restrain the core effectively, the steel tube was connected with the core through spot welds on midpoint of longitude direction of the BRB for the specimen used in the uniaxial tests, as shown in Fig.1.

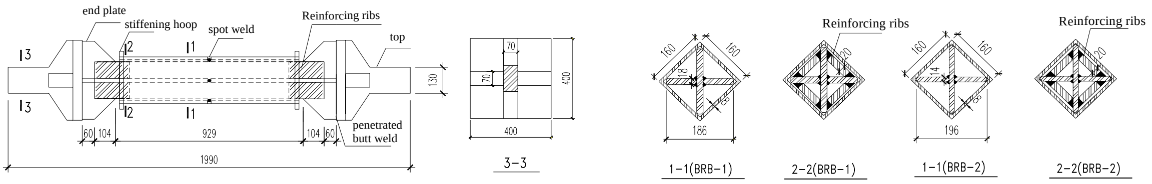

Figure 1 Configuration of BRB-1 and BRB-2

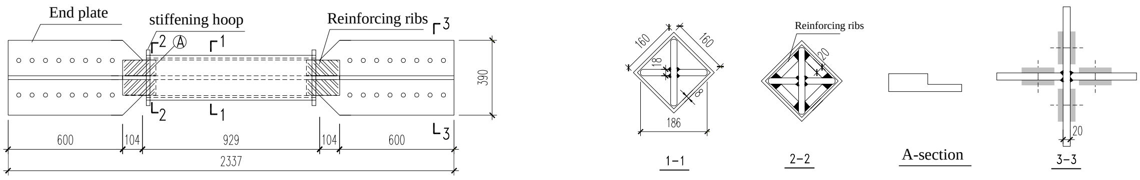

Figure 2 Configuration of BRB-3

2.3. Design Parameters of BRBs

The parameters of the specimens are summarized in Table 2.1, where A_y represents the cross section area of the core, A_1 represents the cross section area of the core with reinforcing ribs, A_2 represents the cross section area of the end plate, A_1/A_y and A_2/A_y are larger than one to keep the core ends and the end plates within elastic range respectively, and *b/t* is width to thickness ratio of the core. *b* and *t* are shown in Fig3. P_e represents Euler critical load of the outer tube. P_y is the tested yielding force. The small gap δ between the core member and the confining tube, as shown in Fig. 3, should be provided in order to accommodate the transversal deformation of the core plate due to Poisson's effect under compressive loads. The calculated dimension of the gap for the specimen in this paper was 1.6 mm at each side (Ma, 2008).

Table 2.1 Parameters of the specimens

Specimen No.	A_y(mm^2)	A_1/A_y	A_2/A_y	b/t	P_e/P_y	δ(mm)
BRB-1	6372	1.93	2.39	4.7	8	~2
BRB-2	5292	2.12	2.88	6.5	9	~2.5
BRB-3	6372	1.93	2.39	4.7	8	~1.7

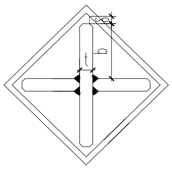

Figure 3 The gap between the core and the outer tube

3. UNIAXAIL TESTS

The full-scale uniaxial test was done at the structural engineering laboratory of Harbin Institute of Technology by MTS actuator with a capacity of 2500kN in compression and in tension. To more accurately measure the relative displacement between the two ends of the steel core, two potentiometers (LVDT-1 and LVDT-2) were set on each side of the specimen in vertical plane. The setup is shown in Fig.4.

BRB-1 was subjected to an increasing-amplitude quasi-static cyclic loading history, as shown in Table 3.1 and illustrated in Fig.5

Table 3.1 Loading parameter of BRB-1

Loading step No.	Story drift (%)	Target displacement (mm)	Target strain (%)	No. of cycle
1	0.375	9.3	1.3	6
2	0.5	12.4	1.7	6
3	0.75	18.6	2.6	6
4	1.0	24.7	3.4	4

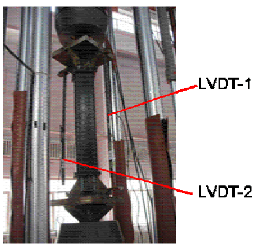

Figure 4 Photo of uniaxial test setup of BRB-1

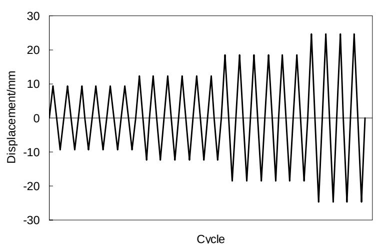

Figure 5 Loading history of BRB-1

During the loading process, the rotation of the top end of the specimen was observed when the actuator displacement reached 18.6mm under the maximum compression load. Meanwhile, the pointer of LVDT-1 was bent heavily. This may be attributed to the initial eccentricity caused by the machining errors. For the purpose of protecting the MTS, the test was terminated. The hysteretic loops are shown in Fig.6.

In Fig.6, a plastic platform can be observed during the first tensile loading. The maximum displacement of the platform is four times of the yielding displacement, and the corresponding yielding force is 1850kN. It is 40% larger than 1338kN, which was calculated from the result of the material test. The phenomenon was resulted from the welding of the core plate.

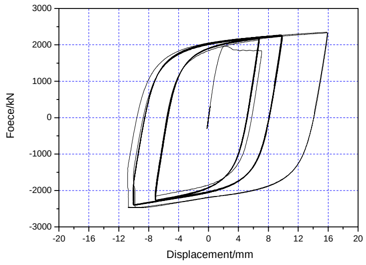

Figure 6 Hysteretic curves of BRB-1

According to the test result of BRB-1, the cross section area of BRB-2 was reduced to satisfy the requirement of the yielding force. The machining accuracy of the BRB-2 was improved to reduce the initial eccentricity of the brace. Two additional potentiometers (*i.e.* LVDT-3 and LVDT-4) were set horizontally on the top and bottom end of the brace to monitor the rotation of the two ends, as shown in Fig.7.

The loading history of BRB-2 is shown in Table 3.2 and Fig8. Compared with the testing protocol for BRB-1, the amplitude of control displacement was adjusted to account for the deformation of the loading frame.

Table 3.2 Loading parameter of BRB-2

Loading step No.	Story drift (%)	Control displacement (mm)	Target displacement (mm)	Target strain (%)	No. of cycle
1	0.375	12	9.27	1.3	6
2	0.5	15.4	12.36	1.7	6
3	0.75	21.2	18.54	2.6	6
4	1.0	27.4	24.72	3.4	4

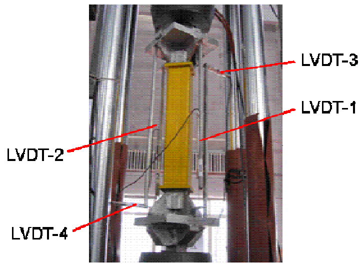

Figure 7 Photo of uniaxial test setup of BRB-2

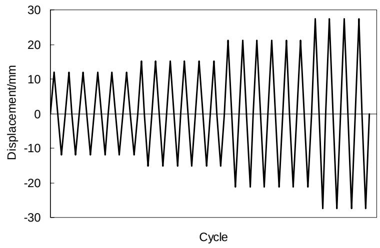

Figure 8 Loading history of BRB-2

Due to improvement of machining accuracy, the rotation angle of BRB-2 was small during the loading process. BRB-2 performed well up to the compression load of nearly 2500kN. The test was paused because of the capacity limit of the actuator. The actuator was reset to its original position, and then the tensile force was applied. The tensile force of the BRB-2 started to drop at the displacement of 20mm (Fig.9), indicating occurrence of fracture, so that the test was stopped. Then, BRB-2 was taken apart in order to examine its failure pattern. As shown in Fig.10, the core plates broken along the cross section at the weld spots connecting the core and outer tube. The reason for this was the local welding on the yielding part of the core which deteriorated the low cycle fatigue property of the brace. It indicates that, for better performance, there should be no additional weld within the yielding region of the core except the welding to form a cruciform section.

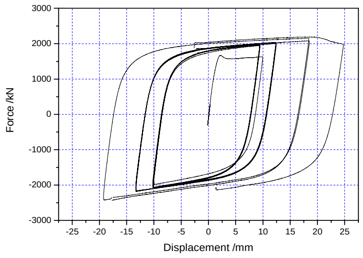

Figure 9 Hysteretic curves of BRB-2

Figure 10 Rupture of the core plates

4. SUBASSEMBLAGE TEST

4.1. Test System and Loading Protocol

According to the experience obtained in the uniaxial tests, for the specimen used in subassemblage test which included BRB-3 and gusset plates, the portion of rectangle reinforcing ribs outside of the outer tube were thickened instead of weld to restrain the slippage of the tube, as shown in Fig.2 and Fig.11.

The full-scale subassemblage test was done in the structural engineering laboratory in Shenyang Jian Zhu University. Figs.12 show the photo of the subassemblage test system, the configuration of which was intended to represent the geometry and loading conditions for braces used in the practical project. The top end of the column was loaded horizontally by two hydraulic actuators that fixed against a vertical reaction wall, and the other end was pinned with the beam base, which were anchored to the strong floor of the laboratory. The gusset plate was connected to the column and the beam base with full penetration welds which was exactly the same as the actual structure. The brace bolted to the gusset plate, which was also identical with the connection form in the actual structure. Because of the machining error, the bottom gusset plate in the test had a visible initial out of plane inclination. In order to restrict the out-of-plane deformation of the loading frame, two lateral supports were set at each side of the column. Each of the actuators (MTS) had capacities of 960kN in tension and 1500kN in compression, thus the total horizontal tension force and compression force given by them were 1920kN and 3000kN, respectively. Besides, they had displacement capacity of ±250mm. Two wire potentiometers were set on each side of the brace in an inclination plane to measure the relative displacement between the two ends of the steel core.

Figure 11 Photo of BRB-3

Figure 12 Photo of the subassemblage test system

BRB-3 was subjected to an increasing-amplitude cyclic loading history, as shown in Table 4.1 and illuminated in Fig.13, at a velocity of 0.3mm/s. This loading sequence contained six cycles at the story drift of 0.25%, 0.5%, 0.75% and three cycles at the story drift of 1.0%. The target axial deformation was calculated by story drift. The horizontal displacement of the actuators was taken as control loading-parameter including the gap in the hinge.

Table 4.1 Loading parameter of BRB-3

Loading step No.	Story drift (%)	Target axial deformation (mm)	Control horizontal displacement (mm)	Target core strain (%)	No. of cycle
1	0.25	6.2	15	0.9	6
2	0.5	12.4	24	1.7	6
3	0.75	18.6	33	2.6	6
4	1.0	24.8	42	3.4	4

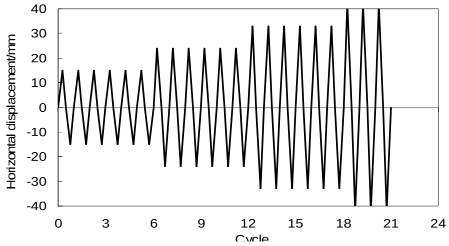

Figure 13 Loading history of BRB-3

4.2. Results

4.2.1 Test phenomena

The test was carried out under the loading protocol and it had been found no rupture in the process. Then we decided to apply additional cyclic loading, the control horizontal displacement of which was 51mm corresponding to 1.25% peak story drift. The brace performed well in the first cycle under the load, but slight out-of-plane deformation had been observed at the bottom gusset plate and the bottom end plate of the brace under the maximum compression load in the second cycle. The deformation resulted from the large out-of-plane moment caused by the initial eccentricity caused by obvious machining error of the gusset plate and the axial load of nearly 3000kN. Nevertheless, the test was continued to observe the damage pattern. The deformation occurred in the subsequent cycle at approximately the same axial compression load until the actuator load dropped at the maximum compression in the fourth cycle at the story drift of 1.25%. The cyclic test was therefore stopped.

As shown in Fig.14a, large deformation was observed on the bottom gusset plate and the bottom end plate of the specimen. The right side of the bottom gusset plate buckled out of plane was shown in Fig.14b, and the lacquer on the gusset plate was peeled off. In addition, the large local deformation of the connection plate between the brace end plate and the bottom gusset plate was visible (Fig.14c). The bending deformation of the brace was concentrated on the bottom end of the core (Fig.14a) and this caused the distortion of the stiffening hoop, as shown in Fig.14d. Because the top gusset plate and the brace end hadn't been damaged during the whole test, the failure mode was probably caused by the initial construction error of the bottom gusset plate.

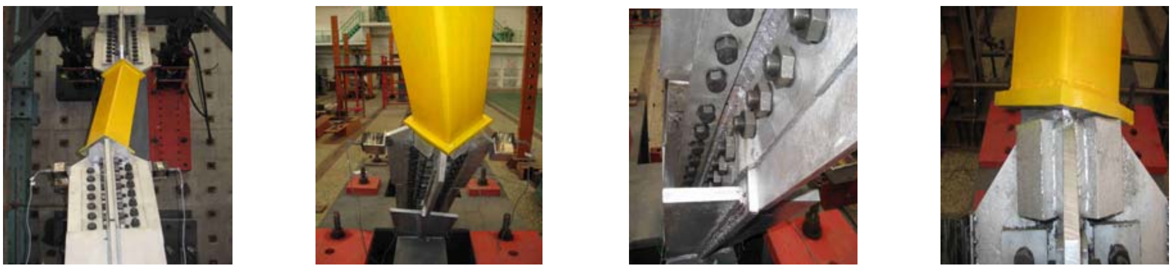

(a) deformation of the brace End　(b) buckling of the gusset plate　(c) deformation of the connection plate　(d) distortion of the stiffening hoop

Figure 14 The failure of BRB-3

After the testing, the specimen was taken apart in order to examine the steel core plate. Some photos are presented in Fig.15. As shown in Fig.15a, the bottom end of the steel core was curved. The local buckling observed on the plate of the bottom end core was caused by the out-of-plane deformation of the brace end (Fig.15b). The higher-mode buckling wave in the middle segment of the core plate was not obvious and the amplitude was smaller than that of BRB-2 (Fig.15c), which indicates the gap between the steel core and the restraining tube is appropriate.

(a) bending deformation of bottom end (b) local buckling of the core (c) deformation at the yielding part

Figure 15 The brace core after the test

4.2.2 Discussion of the result

Fig.16 plots the brace axial force versus axial displacement for the specimen. The axial force was inclined component of applied horizontal force. It is seen from Fig.10 that the specimen showing rich hysteretic loops exhibited stable energy absorption capacity without any degradation of stiffness and strength for the brace during all cycles of incremental amplitude loading. The brace core exhibited maximum longitudinal strains of about 3.2%. No tension rupture occurred according to the figure, which was different from the behavior of the brace in the uniaxial test conducted before. The results further showed that there should be no additional weld within the yielding region of the core except the welding to form a cruciform section. The core with the reinforcing ribs hadn’t been damage. The reinforcing ribs which section area is almost equal to the section area of the core can prevent outside-tube segment of the core from local buckling effectively. The end plate which section area is about 1.5 times larger than that of core performed well without any torsion buckling.

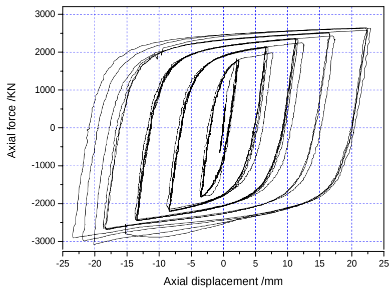

Figure 16 Hysteretic curves of BRB-3

The maximum tension and the maximum compression under the stable cycle of each loading step are listed in Table 4.2. The compression strength adjustment factor β defined as the ratio of the corresponding maximum compression force to the maximum tension force in the same cycle is between 1.0 and 1.1. Because the maximum axial deformation in compression is a little lager than that in tension due to the gap in the hinge, the corresponding maximum compression force indicates the compressive axial load with the same absolute value of the maximum axial deformation in tension. The reason for the maximum compression force being larger than the maximum tension force is that the contact force between the core plate and encasing tube in compression become increasingly larger with small-amplitude buckling wave occurring. Besides, the increase of strength resulted from Poisson’s effect is also an important reason. The maximum β value is 1.1, which is smaller than the limiting value of 1.3 in the SEAOC-AISC Recommended Provisions, and it indicates the friction between the steel core and the outer tube is not significant due to the reasonable width of the gap. It is also found in Table 4.2 that β increased with the increase of axial force. It is because the friction force became larger with increasing amount of buckling waves resulted from the increase of axial force. The specimen exhibited good ductility and good low cycle fatigue behavior with the cumulative inelastic ductility factor of 720 which is much larger than the requirement of 200 in the SEAOC-AISC Recommended Provisions.

Table 4.2 Loading parameter of BRB-3

Loading step No.	1	2	3	4	5
Max tension P_t (kN)	1783	2143	2361	2631	2630
Max compression P_c (kN)	1825	2211	2452	2686	2902
Compression strength amplification factor β (P_c/P_t)	1.02	1.03	1.04	1.06	1.1

5. CONCLUSION

Based on the full scale uniaxial and subassemblage test and analysis, summary and conclusions are made as follows.

1) The all-steel BRB with cruciform cross section encased in a square steel tube in the subassemblage test presented high energy dissipation capacity and stable hysteretic behavior.

2) There should be no additional weld on the yielding part of the core except the necessary connection between the core plates; otherwise the low cycle fatigue property of the brace will decrease.

3) The machining error of BRB and installation error of gusset plates which may deteriorate the hysteretic behavior of the brace should be strictly kept in a tolerable range.

ACKNOWLEDGEMENTS

This research is financial supported by the National Basic Research Program of China (973 Program) (2007CB714204) and the National Key Technology R&D Program (2006BAJ03B06 and 2006BAJ03B03). Great help and support provided by Professors Lianguang Jia, Yafeng Xu, Peiyuan Xu and other laboratory personnel at Shenyang Jian Zhu University, Yunfei Ma and Yong Wu at Harbin Institute of Technology are gratefully acknowledged.

REFERENCES

Black, C. J., Makris, N. and Aiken, I. D. (2004). Component Testing, Seismic Evaluation and Characterization of Buckling-restrained Braces. *Journal of Structural Engineering* **130:6,** 880-894.

Iwata, M. and Murai M. (2006). Buckling-restrained Brace Using Steel Mortar Planks; Performance Evaluation as a Hysteretic Damper. *Earthquake Engineering and Structural Dynamics* **35:** 1807-1826.

Kimura, K., Yoshizaki, K.and Takeda, T. (1976). Tests on Braces Encased by Mortar Infilled Steel Tubes. *Summaries of Technical Papers of Annual Meeting*, 1041~1042.

Ma, N., Wu, B., Zhao, J.X., Li, H., and Ou, J.P. (2008). Full Scale Uniaxial Tests on Earthquake Resistant Behaviour of All-steel Buckling-restrained Brace. *The Seventeenth National Conference on Structural Engineering,* Wuhan, China (Accepted)

Tsai, K.Q., Loh, C.H., Hwang, Y.Z., and Weng, C.S. (2003).Seismic Retrofit of Building Structures with Damper in Taiwan. *Symposium of Seismic Retrofit of Buildings and Bridges with Base Isolation and Dampers*, Kyoto, Japan.

Xie, Q. (2005). State of the Art of Buckling-restrained Braces in Asia. *Journal of Construction Steel Research* **61:** 727-748.